Int. J. Heat Mass Transfer. Vol. 31, No. 3, pp. 591–602, 1988
Printed in Great Britain

0017–9310/88 $3.00 + 0.00
Pergamon Press plc

On the mass transfer in a circular conduit dialyzer when ultrafiltration is coupled with dialysis

M. ABBAS and V. P. TYAGI

Division of Biomechanics, Department of Biological Engineering, U.T.C., BP 233, 60206 Compiègne Cedex, France

(*Received* 27 *October* 1987)

Abstract—Transport of a solute in a laminar flow of a Newtonian fluid through a permeable circular duct, where there exists a small radial flux of the fluid (ultrafiltration) at the duct wall, is considered theoretically. Assumptions are made which are satisfied in a test-dialyzer. An exact analytical solution for the concentration profile is obtained by using separation of variable method. The necessary requirement that the solution must tend to the pure dialysis case solution in the limit ultrafiltration tending to zero is fulfilled. Exact analytical expressions are derived for the eigenconstants of the solution. This solution is applied to blood flow mass transfer in a hollow fibre artificial kidney performing simultaneous dialysis and ultrafiltration. Comparisons are made with earlier work.

1. INTRODUCTION

STEADY state heat and mass transfer problems of incompressible laminar flows in circular and flat ducts have been studied theoretically by a large number of investigators, as these problems are both of fundamental and technological importance. In the present paper, we consider the steady state mass transfer in a homogeneous fluid which flows through a straight circular duct. The mass transfer entrance region is preceded by a part of the duct in which the fluid flow gets fully developed. In the fluid medium in the duct, mass transfer occurs due to diffusion (dialysis) and convection (ultrafiltration) of a solute across the membrane (duct wall) to another fluid called the dialysate, where the dialysate is a solvent that flows outside the duct and flows fast and with mixing. In the part of the duct where mass transfer occurs, the flow is laminar and is assumed to be Newtonian and of constant physical properties. It is assumed that axial mass diffusion is negligible and that dialysate side mass transfer resistance and bulk concentration, ultrafiltration velocity at duct wall and mass transfer entrance section concentration are constant. The mass flux to the inner surface of the duct wall is equal to the mass flux through the wall.

This work is motivated by the blood flow mass transfer problem occurring in a hollow fibre artificial kidney that performs dialysis and ultrafiltration simultaneously. With regard to artificial kidney, simultaneous dialysis and ultrafiltration (SDF) is of current interest. This SDF procedure provides adequate removals of both small molecules (low molecular weight toxic molecules) and middle molecules (intermediate molecular weight toxic molecules) from uremic blood, which is not possible by dialysis or ultrafiltration alone. According to clinician's review [1] and clinical experiences of Leber *et al.* [2] and Wizemann *et al.* [3], the SDF procedure is well tolerated by the patients and reduces the treatment time.

Successful rigorous theoretical studies [4–6] on the above-stated mass transfer problem are available, but for its particular case of zero ultrafiltration, i.e. for the case of pure dialysis. Jagannathan and Shettigar [7] attempted to provide a rigorous theoretical study on the problem in the case of SDF, but their work is open to discussion as will be shown later. The present paper is concerned with a new approach to the problem of combined dialysis and ultrafiltration stated above. As compared to the earlier work [7], some of the features of the present study are as follows.

(1) An appropriate non-dimensionalization scheme is used.

(2) A correct expression for axial velocity component from Yuan and Finkelstein [8] is used.

(3) An analysis is given from which pure dialysis case results are deducible as a limiting case of zero ultrafiltration.

(4) Exact analytical expressions for eigenconstants under variable separable method are obtained.

2. ANALYSIS

Using the cylindrical polar coordinates $(\bar{r}, \theta, \bar{x})$ for the interior of the circular duct, the equations governing the mass transfer problem in hand may be written as follows.

The mass balance equation:

$$D\left[\frac{\partial^2 c}{\partial \bar{r}^2}+\frac{1}{\bar{r}}\frac{\partial c}{\partial \bar{r}}\right]=\bar{u}\frac{\partial c}{\partial \bar{x}}+\bar{v}\frac{\partial c}{\partial \bar{r}}. \quad (1)$$

The initial condition:

$$c=c_i \quad \text{at } \bar{x}=0. \quad (2)$$

The boundary condition:

$$-D\frac{\partial c}{\partial \bar{r}}+\bar{V}_w c=K_w(c-c_D)+T_R\bar{V}_w c$$

$$\text{at } \bar{r}=R, \quad \bar{x}>0. \quad (3)$$

NOMENCLATURE

a_{2n}	series coefficients introduced by equation (27)	R	hollow fibre radius
A_m	eigenconstants introduced by equation (32)	R_D	dialysate side mass transfer resistance
B	parameter given by equation (10)	R_u	ultrafiltration Reynolds number
c	local concentration	Sh_w	wall Sherwood number
c_D	bulk dialysate concentration	T_R	membrane transmittance coefficient
c_i	mass transfer entrance section concentration	u	dimensionless form of $\bar{u}$
c_M	mixing-cup concentration	u_m	$\bar{u}_m/\bar{u}_m(0)$
c_{mid}	central line concentration	$\bar{u}$	velocity component in x-direction in dialyser
c_w	wall concentration	$\bar{u}_m$	mean of $\bar{u}$
D	diffusivity coefficient	$\bar{u}_m(0)$	$\bar{u}_m$ at $x = 0$
F	dimensionless form of c	v	dimensionless form of $\bar{v}$
K_w	wall mass transfer coefficient, $(1/(R_D+1/P_m))$	V	ultrafiltration rate
L	dialyzer length	$\bar{v}$	velocity component in r-direction in dialyser
N_h	number of hollow fibres	$\bar{V}_w$	ultrafiltration velocity
p	function given by equation (33)	x	dimensionless form of $\bar{x}$
P_m	membrane permeability	x_L	value of x at $x = L$
Q	flow flux in dialyzer	$\bar{x}$	axial coordinate
Q_i	value of Q at mass transfer entrance section	X	function introduced by equation (21)
r	dimensionless form of $\bar{r}$	Y	function introduced by equation (21).
$\bar{r}$	radial coordinate under cylindrical polar coordinate system, with origin at the centre of mass transfer entrance section	Greek symbols	
		β_m	eigenvalues
		θ_D	c_D/c_i
		ν	kinematic viscosity
		ψ	ultrafiltration Peclet number.

The natural boundary condition:

$$\frac{\partial c}{\partial \bar{r}} = 0 \quad \text{at } \bar{r} = 0. \tag{4}$$

The axial velocity component $\bar{u}$ and the radial velocity component $\bar{v}$, according to Yuan and Finkelstein [8], are given by

$$\bar{u} = 2\bar{u}_m(0)\left[\frac{1}{1+\frac{1}{18}\left(\frac{\bar{V}_w R}{\nu}\right)} - \frac{2\bar{V}_w}{\bar{u}_m(0)}\cdot\frac{\bar{x}}{R}\right]\left[1-\left(\frac{\bar{r}}{R}\right)^2 - \left(\frac{1}{36}\right)\left(\frac{\bar{V}_w R}{\nu}\right)\left\{-2+9\left(\frac{\bar{r}}{R}\right)^2 - 9\left(\frac{\bar{r}}{R}\right)^4 + 2\left(\frac{\bar{r}}{R}\right)^6\right\}\right] \tag{5}$$

$$\bar{v} = \frac{2\bar{V}_w}{\left(\frac{\bar{r}}{R}\right)}\left[\left(\frac{\bar{r}}{R}\right)^2 - \frac{1}{2}\left(\frac{\bar{r}}{R}\right)^4 - \left(\frac{1}{72}\right)\left(\frac{\bar{V}_w R}{\nu}\right) \times \left\{-4\left(\frac{\bar{r}}{R}\right)^2 + 9\left(\frac{\bar{r}}{R}\right)^4 - 6\left(\frac{\bar{r}}{R}\right)^6 + \left(\frac{\bar{r}}{R}\right)^8\right\}\right]. \tag{6}$$

It may be noted that the above equations with ultrafiltration velocity $\bar{V}_w = 0$ refer to pure dialysis [4–6].

We use the following non-dimensionalization scheme:

$$x = \frac{\bar{x}D}{2R^2\bar{u}_m(0)}, \quad r = \frac{\bar{r}}{R} \tag{7}$$

$$u = \frac{\bar{u}}{\bar{u}_m(0)}, \quad v = \frac{\bar{v}}{\bar{V}_w} \tag{8}$$

$$F = \frac{(c-c_i B)}{(c_i - c_i B)} \tag{9}$$

where

$$B = \frac{c_D Sh_w}{c_i[Sh_w - (1-T_R)\psi]} \tag{10}$$

$$Sh_w = \frac{K_w R}{D} \tag{11}$$

$$\psi = \frac{\bar{V}_w R}{D}. \tag{12}$$

(The parameter Sh_w is the wall Sherwood number and the parameter ψ is the ultrafiltration Peclet number.)

In terms of the above-defined dimensionless quantities, the system of basic equations (1)–(6) transforms to

$$\frac{\partial^2 F}{\partial r^2}+\frac{1}{r}\frac{\partial F}{\partial r}=\frac{u}{2}\frac{\partial F}{\partial x}+\psi v\frac{\partial F}{\partial r} \tag{13}$$

$$F=1 \quad \text{at } x=0 \tag{14}$$

$$\frac{\partial F}{\partial r}+[Sh_w-(1-T_R)\psi]F=0 \quad \text{at } r=1, \quad x>0 \tag{15}$$

$$\frac{\partial F}{\partial r}=0 \quad \text{at } r=0 \tag{16}$$

$$u=\frac{1}{E_1}(1-4E_1\psi x)g, \quad v=\frac{2}{r}f,$$

$$u_m=\frac{1}{E_1}(1-4E_1\psi x) \tag{17}$$

where

$$g=2\frac{df}{d(r^2)}, \quad f=(E_1r^2-E_2r^4+E_3r^6-E_4r^8) \tag{18}$$

$$E_1=1+\frac{R_u}{18}, \quad E_2=\frac{1}{2}+\frac{R_u}{8}, \quad E_3=\frac{R_u}{12}, \quad E_4=\frac{R_u}{72} \tag{19}$$

$$R_u=\frac{\bar{V}_w R}{\nu}. \tag{20}$$

(The parameter R_u is the ultrafiltration Reynolds number.)

If we set $R_u=\psi=0$ in the above dimensionless equations (13)–(19), we obtain those of pure dialysis case. This is not found with the study of Jagannathan and Shettigar [7].

Using variable separable method and, hence, taking

$$F=X(x)Y(r) \tag{21}$$

equations (13), (15) and (16) are reduced to

$$\frac{1}{E_1}(1-4E_1\psi x)X'+\beta^2X=0 \tag{22}$$

$$Y''+\left(\frac{1}{r}-\psi\frac{2}{r}f\right)Y'+\beta^2\left(\frac{g}{2}\right)Y=0 \tag{23}$$

$$Y'+[Sh_w-(1-T_R)\psi]Y=0 \quad \text{at } r=1 \tag{24}$$

$$Y'=0 \quad \text{at } r=0 \tag{25}$$

where β is an unknown parameter and is required to be determined.

Equation (22) has as its solution

$$X=(1-4E_1\psi x)^{\beta^2/4\psi}. \tag{26}$$

A solution to equation (23), subject to the boundary conditions (24) and (25), can be obtained by the Frobenius method, i.e. by taking

$$Y=\sum_{n=0}^{\infty}a_{2n}r^{2n} \tag{27}$$

which, when substituted back into equation (23), admits the following values for the constants a_{2n}:

$$a_0=1$$

$$a_{2i+8}=\frac{1}{(2i+8)^2}[\{(4i+12)\psi-\beta^2\}E_1a_{2i+6}+\{2\beta^2-(4i+8)\psi\}E_2a_{2i+4}+\{(4i+4)\psi-3\beta^2\}\times E_3a_{2i+2}+\{4\beta^2-(4i)\psi\}E_4a_{2i}] \tag{28}$$

where

$$i=-3,-2,-1,0,1,2,\ldots$$

$$a_{-2}=a_{-4}=a_{-6}=0 \tag{29}$$

and satisfies equation (24) by demanding

$$\sum_{n=0}^{\infty}[2n+Sh_w-(1-T_R)\psi]a_{2n}=0. \tag{30}$$

The roots of equation (30), denoted by β_m, $m=1,2,\ldots$, are the eigenvalues.

In using the initial condition given by equation (14), the solution for the system of equations (13)–(16) is given as follows:

$$F=\sum_{m=1}^{\infty}A_mX_mY_m \tag{31}$$

where X_m denotes X and Y_m denotes Y when β denotes β_m and the coefficients A_m, called eigenconstants, are given by

$$A_m=\frac{\int_0^1\exp(p)\left(\frac{g}{2}\right)Y_m\,dr}{\int_0^1\exp(p)\left(\frac{g}{2}\right)Y_m^2\,dr}, \quad m=1,2,\ldots, \tag{32}$$

with

$$p=\int\left(\frac{1}{r}-\psi\left(\frac{2}{r}\right)f\right)dr. \tag{33}$$

The solution for the local concentration, c, is therefore given by

$$c=c_iB+c_i(1-B)\sum_{m=1}^{\infty}\left[A_m(1-4E_1\psi x)^{\beta_m^2/4\psi}\times\left\{\sum_{n=0}^{\infty}a_{2n}^{(m)}r^{2n}\right\}\right] \tag{34}$$

where $a_{2n}^{(m)}$ denotes a_{2n} when β denotes β_m.

The expressions for wall concentration c_w, central line concentration c_{mid} and normall wall concentration gradient $(-\partial c/\partial\bar{r})_{\bar{r}=R}$ are given by (using equation (34))

$$c_w=c_iB+c_i(1-B)\sum_{m=1}^{\infty}\left[A_m(1-4E_1\Psi x)^{\beta_m^2/4\Psi}\times\left\{\sum_{n=0}^{\infty}a_{2n}^{(m)}\right\}\right] \tag{35}$$

$$c_{mid}=c_iB+c_i(1-B)\sum_{m=1}^{\infty}[A_m(1-4E_1\Psi x)^{\beta_m^2/4\Psi}] \tag{36}$$

$$\left(-\frac{\partial c}{\partial \bar{r}}\right)_{\bar{r}=R} = \frac{1}{R}\left[c_i(1-B)\sum_{m=1}^{\infty}\left[A_m(1-4E_1\Psi x)^{\beta_m^2/4\Psi} \times\left\{-\sum_{n=0}^{\infty}2na_{2n}^{(m)}\right\}\right]\right]. \quad (37)$$

By definition, the mixing-cup concentration, denoted by c_M, is to be calculated according to

$$c_M = \frac{\int_0^{2\pi}\int_0^R c\bar{u}\bar{r}\,d\bar{r}\,d\theta}{\int_0^{2\pi}\int_0^R \bar{u}\bar{r}\,d\bar{r}\,d\theta} \quad (38)$$

which under the present non-dimensionalization scheme transforms to

$$c_M = \frac{2}{u_m}\int_0^1 cur\,dr. \quad (39)$$

Using the expressions of c, u and u_m already given in this section, it is found that

$$c_M = c_iB + 2c_i(1-B)\sum_{m=1}^{\infty}\left[A_m(1-4E_1\Psi x)^{\beta_m^2/4\Psi} \times\left\{\sum_{n=0}^{\infty}a_{2n}^{(m)}\left(\frac{E_1}{n+1}-\frac{2E_2}{n+2}+\frac{3E_3}{n+3}-\frac{4E_4}{n+4}\right)\right\}\right]. \quad (40)$$

The computation of the eigenconstants A_m involves a substantial amount of work, as it involves numerical integration (see equation (32)). In fact, Jagannathan and Shettigar [7] also obtained the same type of equation for their eigenconstants and used a numerical method of integration to compute them. Numerical integration can be avoided if one gives an exact analytical solution for the eigenconstants. With reference to this a calculation was done in the present work, where certain operations were performed with equation (23) and equations (24) and (25) were used, and the following exact analytical solution for A_m was obtained:

$$A_m = \frac{-\{Sh_w-(1-T_R)\Psi\}}{\left[\sum_{n=1}^{\infty}\{2n+Sh_w-(1-T_R)\Psi\}\beta^2a'_{2n}\right]_{\beta=\beta_m}}, \quad m = 1, 2, \ldots \quad (41)$$

where

$$a'_{2n} = \frac{da_{2n}}{d(\beta^2)}, \quad n = 1, 2, \ldots. \quad (42)$$

It may be noted that the computer time taken by the above analytical solution for A_m is negligible as compared to that taken by a solution for A_m which involves numerical integration.

The results of the case of pure dialysis are not deducible from the results given in Jagannathan and Shettigar [7], but are easily deducible by setting $R_u = \psi = 0$ in the present results that have appeared after equation (21), excepting the result for X, equation (26), for which mathematical limits are to be evaluated. It is easily obtained that

$$\lim_{\Psi\to 0} X = \exp(-\beta^2 x) \quad (43)$$

where β is to be regarded to be governed by equation (30) with $R_u = \psi = 0$.

3. RESULTS AND DISCUSSION

In this section, some results of Jagannathan and Shettigar [7] are compared with the corresponding results based on the present analysis. Specifically speaking, their Figs. 3, 5 and 6 are referred to in the discussions here. Following Jagannathan and Shettigar [7], the cases of vanishing dialysate bulk concentration and resistance (i.e. $c_D = 0$ and K_w = membrane permeability), which refer to a sufficiently fast dialysate flow with well-mixing, are referred to in the present discussions. The first three figures in the present paper are based on the present analysis and correspond, respectively, to Figs. 3, 5 and 6 of Jagannathan and Shettigar.

Figure 1 shows mixing-cup concentration as a function of x for values of x up to 0.72, whereas, Fig. 3 of Jagannathan and Shettigar shows the same for the values of x up to 0.45. In Fig. 3 of Jagannathan and Shettigar, it is seen that the mixing-cup concentration curves which meet at $x = 0$ are diverging, and that this divergence increases as x increases and is such that it is indicated that the curves are not likely to converge in any sub-range of x. In the present Fig. 1, the mixing-cup concentration curves are seen to converge around $x = 0.45$. It is also observed that the quantitative change that takes place in the mixing-cup concentration in going from zero ultrafiltration to non-zero ultrafiltration is significantly different in Fig. 3 of ref. [7] as compared to the present Fig. 1. This quantitative change is seen to be more in their figure. It is noteworthy that Jagannathan and Shettigar's figure shows that the effect of ultrafiltration is to increase the mixing-cup concentration at all $x > 0$. Therefore, it is interesting that the present Fig. 1 shows that the effect of ultrafiltration is to increase the mixing-cup concentration at all $x > 0$ up to a certain x and then to decrease it at all the remaining higher x. A physical explanation for this may be as follows.

The pure dialysis case mixing-cup concentration shown in the present Fig. 1 is influenced by two factors, namely: (1) wall directed radial fluid motion in the duct; and (2) axial fluid motion reduction everywhere in the region $x > 0$ and increasing of the axial fluid motion reduction with x in the duct, which appear only as a result of ultrafiltration.

The effect of (1) is to increase the mixing-cup concentration, because the fluid that is convected into the wall is convected from the immediate neighbourhood of the wall and the solute concentration in the immediate wall neighbourhood is smaller than that in and around the centre. On the other hand, the effect of (2)

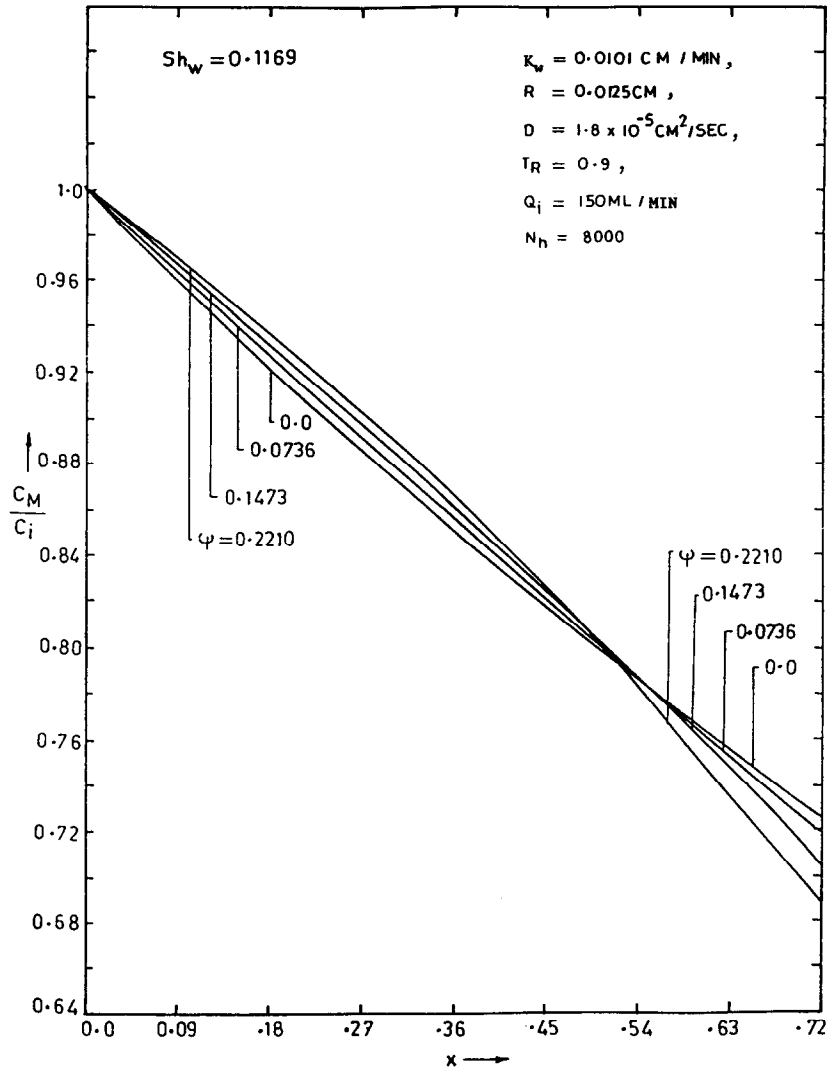

FIG. 1. Mixing-cup concentration vs axial distance for constant Sh_w and various ψ.

is to decrease the mixing-cup concentration, because the lower the axial motion of fluid the lower is the local concentration in the flow field in the duct. The effect of (1) has its maximum intensity near the mass transfer entrance section, $x = 0$, as the concentration differences near the wall are maximum there. On the other hand, the effect of (2) has its minimum intensity near $x = 0$, as axial fluid motion reduction is minimum here. Thus, out of the effects of (1) and (2), the effect of (1) is dominant near $x = 0$. However, the effect of (2) increases as x increases, because the axial fluid motion reduction increases as x increases. Therefore, at a distance away from the mass transfer entrance section in the axial flow direction, the effect of (2) overtakes and dominates that of (1). Thus the given ultrafiltration has the effect of increasing the mixing-cup concentration at all $x > 0$ up to certain x, say, at all x satisfying $0 < x < x_c$, and then that of decreasing the mixing-cup concentration at all the remaining $x > x_c$.

Figure 2 of the present paper shows local concentration as a function of the radial coordinate r at fixed x, namely $x = 0.45$, and for a fixed Sherwood number. In the corresponding Fig. 5 of Jagannathan and Shettigar, the local concentration curves are almost parallel to each other, whereas the present local concentration curves (Fig. 2) are not distinctly parallel. In the present Fig. 2, the curves are close to each other at $r = 0$ and have maximum separation among themselves at $r = 1$. It is also observed that the upward shifting of the local concentration curve, as a result of going from zero ultrafiltration to a non-zero ultrafiltration, in this figure is quantitatively different from that in Fig. 5 of Jagannathan and Shettigar. This upward shifting is significantly smaller in Fig. 2 than in their Fig. 5. Further, their figure shows that local concentration at any r increases, and increases only, with the increase in ultrafiltration velocity, as no two curves of theirs are intersecting. However, the picture with Fig. 2 is somewhat different

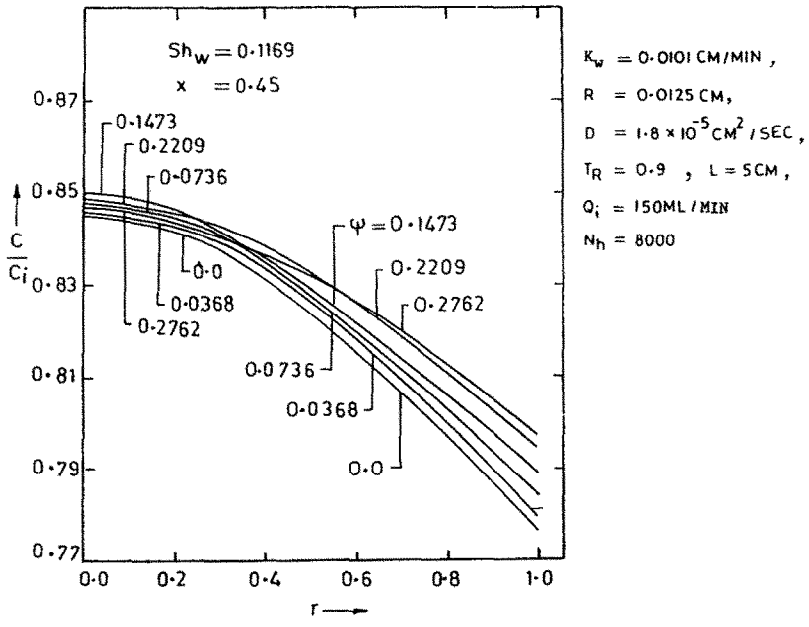

FIG. 2. Local concentration vs radial distance for constant Sh_w and various ψ.

in that some curves are intersecting and the local concentration at any r in a neighbourhood of $r = 0$ decreases with the increase in ultrafiltration velocity if the ultrafiltration velocity is increased beyond a certain value. This may be explained as follows. The wall directed radial fluid motion is smaller in the vicinity of the centre, $r = 0$, than in the vicinity of the wall, $r = 1$. Therefore, the effect of this fluid motion to increase local concentration is less at and around $r = 0$ than at and around $r = 1$. That is one reason that the upward shifting of concentration profile with increments in ultrafiltration velocity in Fig. 2 is less in the vicinity of $r = 0$ than in the vicinity of $r = 1$. Further, as ultrafiltration velocity increases, the effect of the radial fluid motion around the centre, $r = 0$, does not increase as fast as that of axial fluid motion reduction (where the effect of axial fluid motion reduction is to reduce local concentration), particularly at such a distant location as $x = 0.45$. Therefore, if the ultrafiltration velocity is increased beyond a certain value, the local concentration is likely to decrease at and around $r = 0$.

The next figure of the present paper, i.e. Fig. 3, shows local concentration as a function of the radial coordinate r at the same fixed x, i.e. $x = 0.45$, referred to fixed non-zero and zero values of ultrafiltration velocity at various membrane permeabilities. The corresponding Fig. 6 of Jagannathan and Shettigar shows that, at all wall Sherwood numbers, the local concentration is higher in the case of $\psi \neq 0$ than in the case of $\psi = 0$. However, this is true at small Sherwood numbers, which may be explained as follows. As local concentration decreases and nonuniformity in local concentration distribution increases with the increase in membrane permeability, i.e. with the increase in wall Sherwood number, the effect of the axial fluid motion reduction, which is to be felt by, and is to reduce, this concentration, increases as wall Sherwood number increases. As has been mentioned already, this effect also increases with x. Therefore, at such a distant location as $x = 0.45$, the effect of axial fluid motion reduction is likely to become dominant and, therefore, local concentration is likely to be lower in the case of $\psi \neq 0$ than in the case of $\psi = 0$ if wall Sherwood number is increased beyond its certain value. This may be seen in Fig. 3, wherein the concentration profile of the case of $\psi \neq 0$ is below that of the case of $\psi = 0$ when $Sh_w \geqslant 0.3507$.

In the remaining part of this section, we will refer to a specific case. We take $2R = 0.02$ cm and $L = 12$ cm, as these values of hollow fibre diameter and length, respectively, are of interest with reference to modern artificial kidney [1]. With regard to membranes that form walls of hollow fibres, we consider cuprophan (CUP) and polyacrylonitrile (PAN) because they are representative of membranes used in the modern hemodialyzer [9]. As far as solutes are concerned, we take urea and vitamin B-12, as the former is found in the largest quantity among the small molecules in blood and the latter has been recognized as a middle molecule marker [10]. In order to be within clinical limits, as the blood flow rate to, and ultrafiltration rate in, a dialyzer are around 12 and 3 l h^{-1} respectively, we take $\bar{u}_m(0) = 0.53$ cm s^{-1} and three values for the ultrafiltration velocity, viz. $\bar{V}_w = 0.0$, 0.15 and 0.30 cm h^{-1}. The largest value corresponds to $V = 3$ l h^{-1} for a 1 m^2 hemodialyzer. Using these values and $\nu = 1.388 \times 10^{-2}$ cm^2 s^{-1}, the numerical values of wall Sherwood number Sh_w, ultrafiltration Peclet number ψ and ultrafiltration

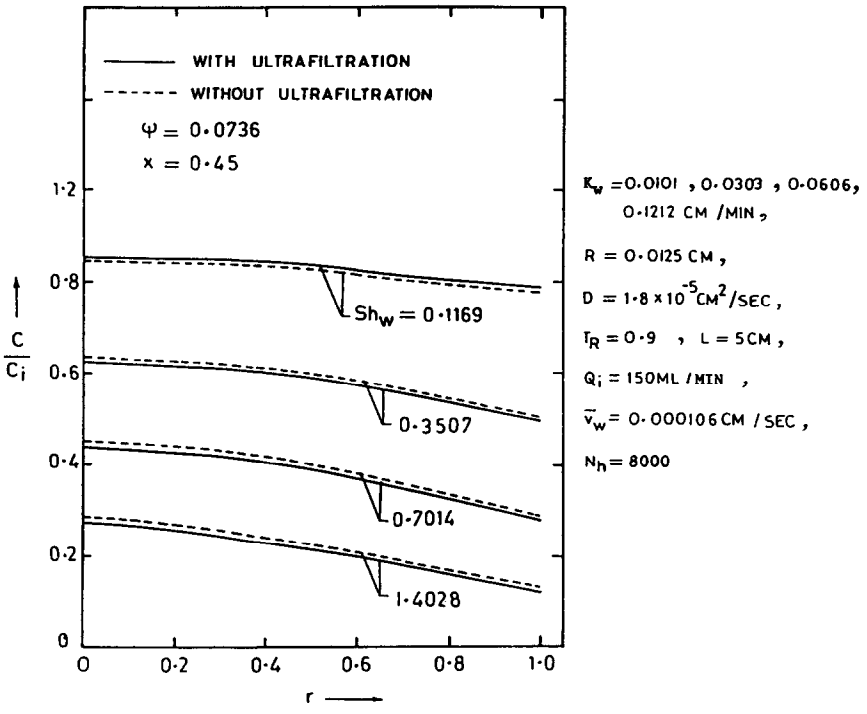

FIG. 3. Local concentration vs radial distance for constant ψ and various Sh_w.

Reynolds number R_u are determined, and are shown in Tables 1 and 2. In Table 1, the references for the values of membrane permeability P_m, diffusivity coefficient D and membrane transmittance coefficient T_R are [10], [11] and [12] respectively.

Figure 4 shows the variation of local concentration with radial coordinate r at three axial locations and for two non-zero ultrafiltration velocities. We note that, in going from pure dialysis to combined dialysis and ultrafiltration, local concentration decreases in the vicinity of centre, i.e. near $r = 0$, and then increases at all remaining higher values of r. However, this behaviour is different at different axial positions.

Figure 5 exhibits the variation of dimensionless normal wall concentration gradient in the main flow direction. It is seen that normal wall concentration gradient decreases as x increases. We observe that this decrease is gradual with the axial coordinate. We also note that in going from zero ultrafiltration to non-zero ultrafiltration the wall concentration gradient is decreased with ultrafiltration velocity.

Figure 6 shows the variation of central line concentration with axial coordinate at different ultrafiltration velocities. It is seen that the central line concentration decreases as x increases. It is also seen that up to a certain axial distance the central line

Table 1. Numerical values of wall Sherwood number and membrane transmittance coefficient

Solutes	Urea		Vitamin B-12	
Membranes	PAN	CUP	PAN	CUP
D (cm^2 s^{-1})	1.0×10^{-5}		0.23875×10^{-5}	
K_w (cm s^{-1})	13.2×10^{-4}	11.5×10^{-4}	2.35×10^{-4}	0.59×10^{-4}
Sh_w	1.32	1.15	0.98429319	0.24712041
T_R	1.0	1.0	0.94	0.629

Table 2. Numerical values of ultrafiltration Peclet and Reynolds numbers

$\bar{V}_w$ (cm h^{-1})	0.0	0.15	0.30
R_u	0.0	0.30019×10^{-4}	0.60038×10^{-4}
ψ (urea)	0.0	0.04166	0.08332
ψ (vitamin B-12)	0.0	0.17452	0.34904

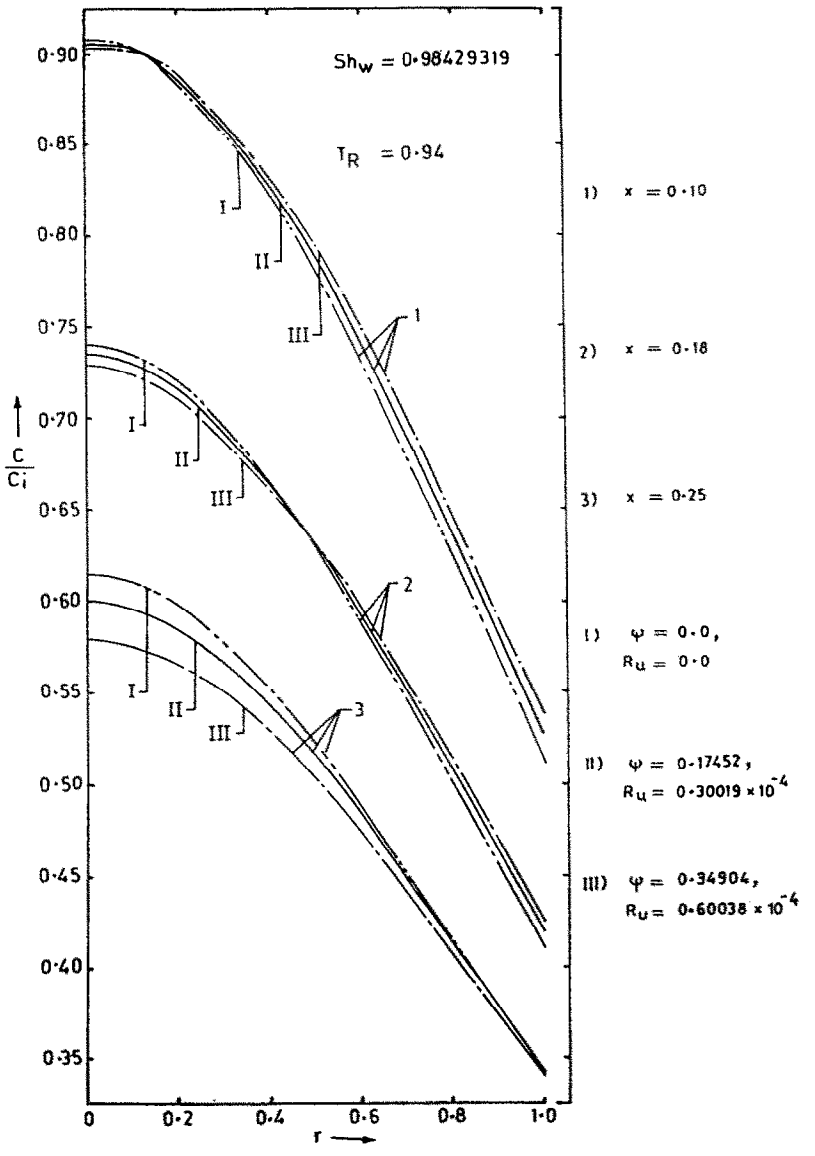

FIG. 4. Local concentration vs radial distance at $T_R = 0.94$ in the cases of vitamin B-12 and polyacrylonitrile.

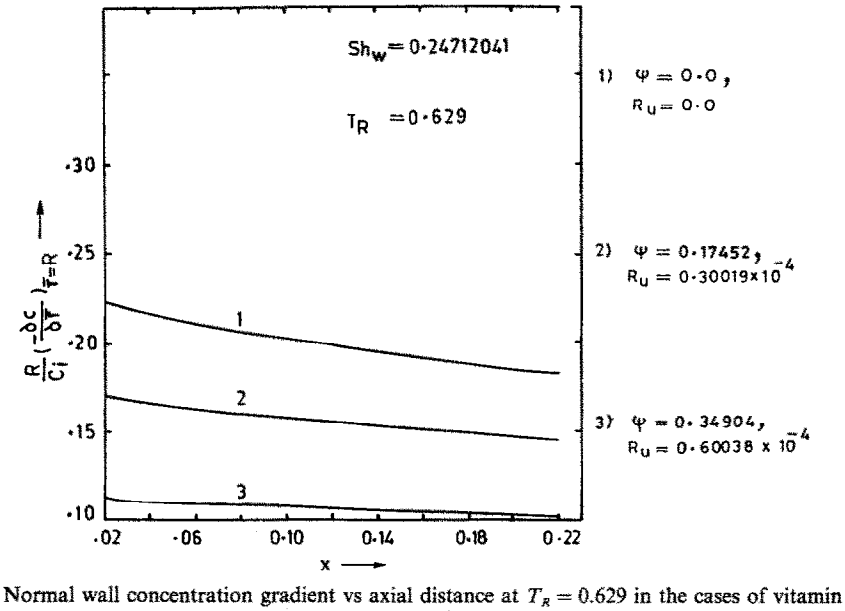

FIG. 5. Normal wall concentration gradient vs axial distance at $T_R = 0.629$ in the cases of vitamin B-12 and cuprophan.

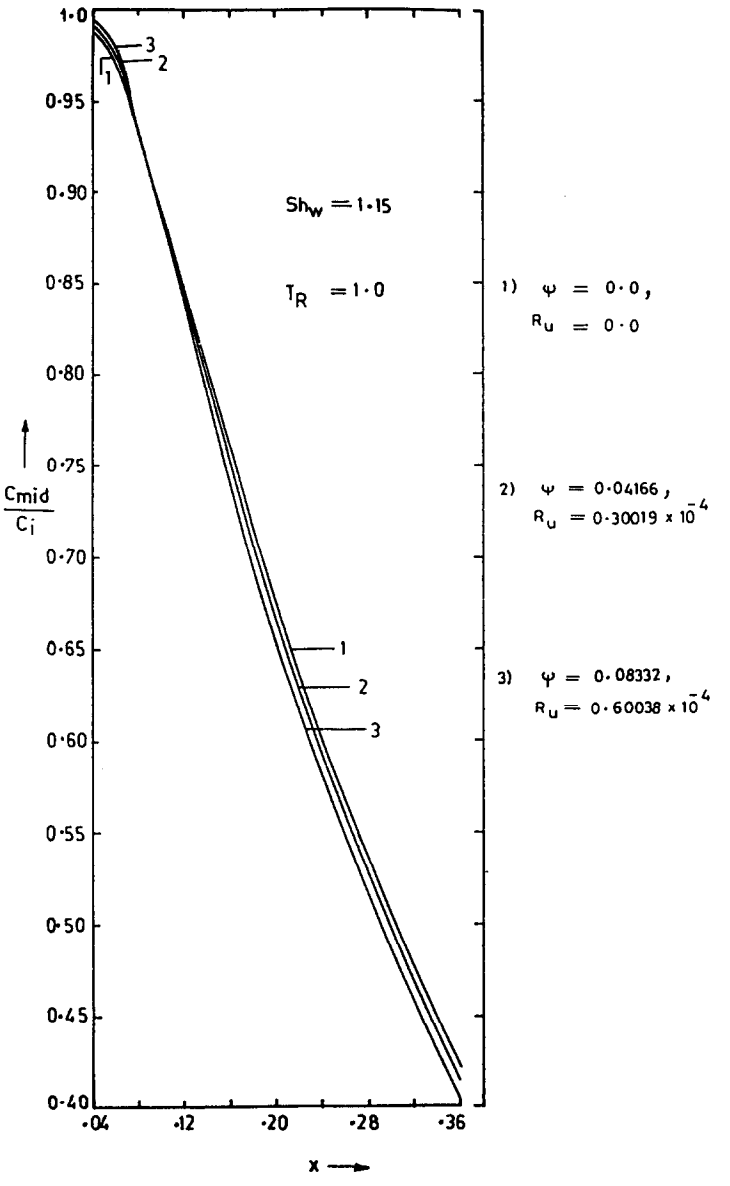

FIG. 6. Central line concentration vs axial distance in the cases of urea and cuprophan.

concentration increases with ultrafiltration velocity, and then it decreases with ultrafiltration velocity at the remaining higher values of x.

Figure 7 exhibits the wall concentration as a function of x. We observe that wall concentration decreases as x increases. It is seen that, due to non-zero $\bar{V}_w$, the wall concentration increases at all x. However, curves reveal that at some higher x the non-zero ultrafiltration may reduce the wall concentration.

Figure 8 shows the dimensionless mixing-cup concentration as a function of x at zero and non-zero ultrafiltration velocities. The value of the mixing-cup concentration in all cases is nearly unity at the mass transfer entrance section, i.e. at $x = 0$.

4. CONCLUDING REMARKS

An exact analytical solution for a steady state solute concentration distribution in a circular duct where mass transfer occurs due to simultaneous dialysis and ultrafiltration has been obtained by using variable separable method. The solution satisfies the necessary requirement that it should yield the solution of the pure dialysis case in the limit ultrafiltration tending to zero. Exact analytical expressions have been obtained for the eigenconstants of the solution, which implies a substantial reduction of numerical work and considerable saving of computer time.

It has been found that the computer time consumed

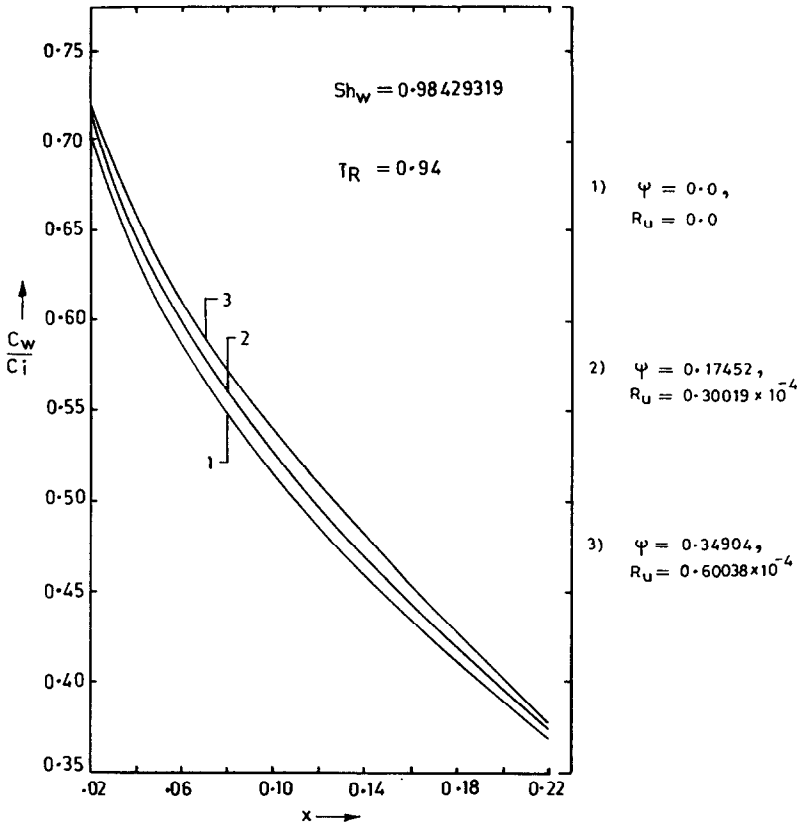

FIG. 7. Wall concentration vs axial distance at $T_R = 0.94$ in the cases of vitamin B-12 and polyacrylonitrile.

by an example of combined dialysis and ultrafiltration is nearly half of that consumed by the corresponding example of pure dialysis.

REFERENCES

1. L. W. Henderson, Current status of hemofiltration, *Artif. Organs* **2**, 120–124 (1978).
2. H. W. Leber, V. Wizemann, G. Goubeaud, P. Rawer and G. Schutterle, Hemodiafiltration: a new alternative to hemofiltration and conventional hemodialysis, *Artif. Organs* **2**, 150–153 (1978).
3. V. Wizemann, P. Rawer, H. Schmidt, E. Techert and G. Schutterle, Efficiency of hemodialysis, hemofiltration and hemodiafiltration, *Hemodiafiltration Proceedings*, Vol. 1, Symposium Giessen, pp. 3–14 (1981).
4. H. R. Davis and G. V. Parkinson, Mass transfer from small capillaries with wall resistance in the laminar flow regime, *Appl. Scient. Res.* **22**, 20–34 (1970).
5. D. O. Cooney, S. S. Kim and E. J. Davies, Analyses of mass transfer in hemodialyzers for laminar blood flow and homogeneous dialysate, *Chem. Engng Sci.* **29**, 1731–1738 (1974).
6. G. Walker and T. Davies, Mass transfer in laminar flow between parallel permeable plates, *A.I.Ch.E. Jl* **20**, 881–889 (1974).
7. R. Jagannathan and U. R. Shettigar, Analysis of a tubular hemodialyzer: effect of ultrafiltration and dialysate concentration, *Med. Biol. Engng Comput.* **15**, 500–511 (1977).
8. S. W. Yuan and A. B. Finkelstein, Laminar pipe flow with injection and suction through a porous wall, *Trans. ASME* **78**, 719–724 (1956).
9. J. E. Sigdell, New products for blood treatment, *Artif. Organs* **9**, 207–208 (1985).
10. E. Klein, J. Autian, J. D. Bawer, G. Buffaloe, L. J. Centella, C. K. Colton, T. D. Darby, P. C. Farrell, F. F. Holland, R. S. Villaroel and R. L. Wathen, Evaluation of hemodialysis and dialysis membranes, Chapter two: *In vitro* characterization of hemodialyzers, *Artif. Organs* **1**, 59 (1971).
11. R. P. Popovitch, T. G. Christopher and A. L. Babb, The effects of membrane diffusion and ultrafiltration properties on hemodialyser design and performance, *Chem. Engng Prog. Symp. Ser.* **67**, 105 (1971).
12. D. M. Green, G. D. Antwiller, J. W. Moncrief, J. F. Dechald and R. P. Popovich, Measurement of the transmittance coefficient spectrum of cuprophan and RP 69 membranes: applications to middle molecule removal via ultrafiltration, *Trans. Am. Soc. Artif. Intern. Organs* **22**, 627–636 (1977).

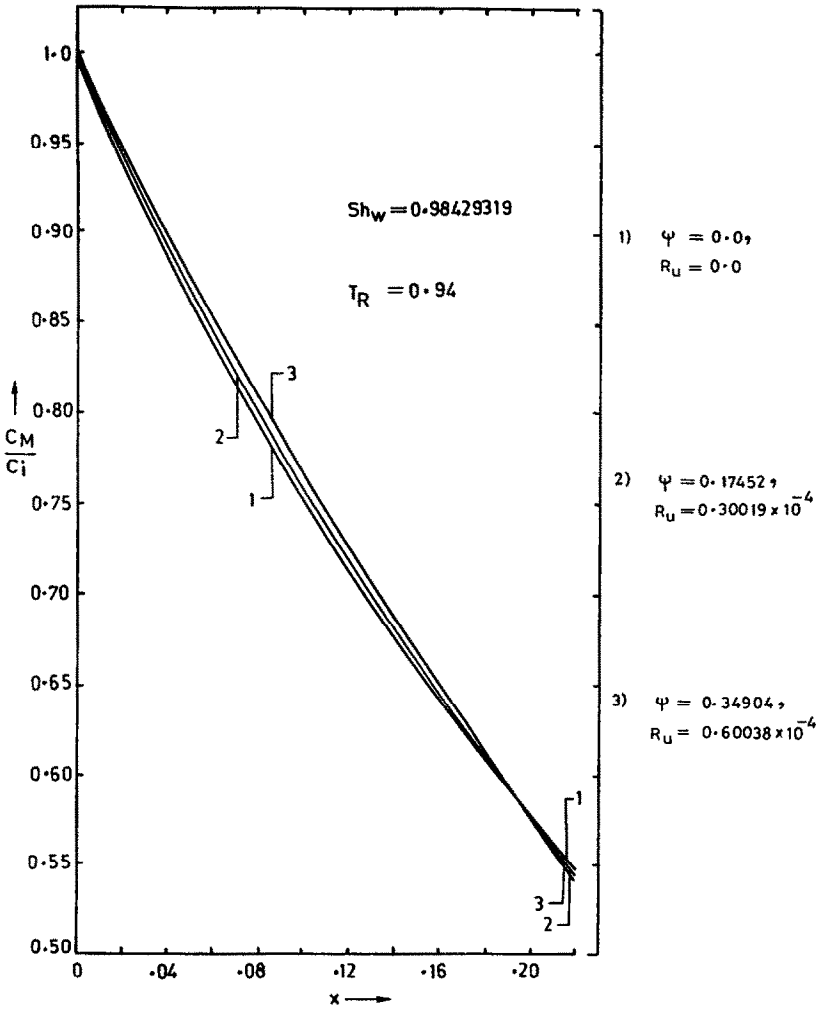

FIG. 8. Mixing-cup concentration vs axial distance at $T_R = 0.94$ in the cases of vitamin B-12 and polyacrylonitrile.

SUR LE TRANSFERT DE MASSE DANS UN DIALYSEUR CYLINDRIQUE LORSQUE L'ULTRAFILTRATION EST COUPLEE AVEC LA DIALYSE

Résumé—On considère théoriquement le transfert d'un soluté dans un fluide newtonien en écoulement laminaire traversant un conduit cylindrique perméable, avec un faible flux radial de fluide (ultrafiltration) à la paroi du conduit. Des hypothèses sont faites qui sont satisfaisantes dans un dialyseur d'essai. Une solution analytique exacte pour le profil de concentration est obtenue en utilisant la méthode de séparation des variables. Elle réduit à la solution de la dialyse pure lorsque l'ultrafiltration tend vers zéro. Des expressions analytiques exactes sont dérivées pour les valeurs propres. Cette solution est appliquée au transfert massique sanguin dans une fibre creuse simulant un rein pour simuler la dialyse et l'ultrafiltration simultanées. Des comparaisons sont faites avec des travaux ultérieurs.

ZUM STOFFAUSTAUSCH IN EINEM RÖHREN-DIALYSATOR BEI GEKOPPELTER ULTRAFILTRATION UND DIALYSE

Zusammenfassung—Der Transport einer Lösung durch ein permeables zylindrisches, von einem newtonschen Fluid laminar durchströmtes Rohr wird theoretisch betrachtet. An der Rohrwand existiert ein kleiner radialer Fluidstrom (Ultrafiltration). Es werden Annahmen gemacht, welche durch Messungen in einem Test-Dialysator gerechtfertigt worden sind. Für das Konzentrationsprofil wird eine exakte analytische Lösung mittels der Trennung der Variablen ermittelt. Die notwendige Forderung, daß die Lösung für den Grenzfall einer verschwindenden Ultrafiltration die reine Dialyse beschreibt, ist erfüllt. Für die Eigenwerte der Lösung werden exakte analytische Ausdrücke hergeleitet. Diese Lösung wird angewendet auf den Stoffaustausch einer Blutströmung durch eine Hohlfaser in einer künstlichen Niere, in der gleichzeitig Dialyse und Ultrafiltration auftritt. Vergleiche mit früheren Arbeiten werden angestellt.

МАССОПЕРЕНОС В КРУГЛОМ ПРОТОЧНОМ ДИАЛИЗАТОРЕ ПРИ ВЗАИМОСВЯЗИ ПРОЦЕССОВ УЛЬТРАФИЛЬТРАЦИИ И ДИАЛИЗА

Аннотация—Теоретически рассматривается перенос растворенного вещества при ламинарном течении ньютоновской жидкости в круглом канале с проницаемыми стенками, через которые происходит небольшое радиальное течение жидкости (ультрафильтрация). Правильность сделанных предположений проверяется на опытном диализаторе. Методом разделения переменных получено точное аналитическое решение для профиля концентраций. Выполнено необходимое условие, согласно которому решение должно стремиться к решению в случае чистого диализа в пределе при стремлении ультрафильтрации к нулю. Для собственных значений постоянных решения получены точные аналитические выражения. Решение использовано применительно к переносу массы при течении крови в пустотелой волокнистой искусственной почке, в которой одновременно происходят процессы диализа и ультрафильтрации. Дано сравнение с результатами ранее проведенного исследования.